C8-1241/501

3

INVESTIGATION OF SINGLE-CRYSTAL FERRITE THIN FILM

By

J. E. Mee
E. C. Whitcomb

and

L. Kolb

June 1968

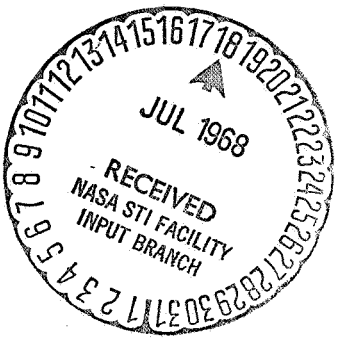

Prepared under Contract No. NAS 12-522 by

Autonetics Division of North American Rockwell Corporation

3370 Miraloma Avenue, Anaheim, California 92803

Electronics Research Center

NATIONAL AERONAUTICS AND SPACE ADMINISTRATION

Howard Lessoff
Technical Monitor
NAS 12-103
Electronics Research Center
575 Technology Square
Cambridge, Massachusetts 02139

INVESTIGATION OF SINGLE-CRYSTAL FERRITE THIN FILM

By

J. E. Mee
E. C. Whitcomb

and

L. Kolb

June 1968

Prepared under Contract No. NAS 12-522 by

Autonetics Division of North American Rockwell Corporation

3370 Miraloma Avenue, Anaheim, California 92803

Electronics Research Center

NATIONAL AERONAUTICS AND SPACE ADMINISTRATION

CONTENTS

ILLUSTRATIONS

C8-1241/501

INVESTIGATION OF SINGLE-CRYSTAL FERRITE THIN FILM

By J. E. Mee, E. C. Whitcomb, and L. Kolb

Autonetics Division of North American Rockwell Corporation
Anaheim, California

SUMMARY

It is the objective of this program to grow and characterize epitaxial lithium ferrite films. The growth method is chemical vapor deposition (CVD).

It was predicted from chemical thermodynamic arguments that lithium halides would be considerably less reactive than iron halides in the proposed deposition reactions. Experimental evaluation of candidate source materials confirmed this prediction and indicated that lithium iodide, LiI, and iron (II) chloride, $FeCl_2$, would be compatible source materials. Reactor conditions were established using these source materials and epitaxial ferrite deposits were obtained on MgO substrates. These deposits had Fe:Li weight ratios ranging from 120:1 to values within experimental error of the desired 40.3:1 ratio. In normal deposition runs, there was a repeatable zone-type behavior in which high Fe:Li deposits were formed first in the reactor and deposits with successively lower Fe:Li ratios were formed "downstream." The deposits were not smooth on {100} and {110} MgO substrates. This appeared to be due to a preferred growth direction which could be resolved by depositing on {111} substrates.

INTRODUCTION

Statement of the Problem

It is of considerable interest to investigate the growth and properties of single-crystal lithium ferrite* films. Lithium ferrite is one of the more interesting and useful ferrites. Because of its high Curie temperature it is superior to other ferrites with respect to temperature stability of parameters used in magnetic logic and memory core applications. It is also promising for certain microwave applications because of its narrow resonance line width and high magneto-elastic coupling constants.

*In this report the name lithium ferrite refers to the ferrimagnetic spinel with the stoichiometry $LiFe_5O_8$, or $Li_{0.5}Fe_{2.5}O_4$ if you prefer. Occasionally in the literature the nonferrimagnetic compound $LiFeO_2$ is also called lithium ferrite. Also in this report, the word ferrite is reserved for the iron-bearing spinel class of ferrimagnetic oxides and does not embrace the ferrimagnetic garnets or magneto-plumbites.

Single crystals of lithium ferrite are needed for material studies and for device applications. It is generally recognized that single crystals are essential for complete characterization of materials. This is especially true for magnetic materials where intrinsic values of properties such as magneto-crystalline anisotropy, magneto-strictive constants, resistivity, and resonance line widths can be definitely determined only by measurements made on the single crystal form of the materials. Domain structure studies on single crystals can give valuable insight into the relative magnitude of various contributions to the total magnetic energy and aid the interpretation of other results. In addition the unique properties of the single crystal form are often necessary for device applications. Single crystals of ferrites or garnets are used in certain microwave devices which utilize the narrow ferromagnetic resonance line width.

Although lithium ferrite crystals have been grown by flux techniques, (Ref 1, 2, 3), other growth techniques need to be used to confirm or correct material properties measured on flux grown crystals. In particular, many magnetic properties are very sensitive to crystal impurity content which is always a concern in flux grown samples. A new technique for growing single crystal metal oxides has emerged in the last few years which is applicable to growth of lithium ferrite crystals. This technique is chemical vapor deposition (CVD). It is most adaptable to growth of thick single crystal films of materials such as ferrites (Ref 4 thru 10), garnets (Ref 11, 12), and simple binary metal oxides (Ref 13). It has also been used to grow good quality, bulk crystals (Ref 14, 15).

Single-crystal lithium ferrite films grown by CVD should meet the requirements of good single crystals for property measurements. But, perhaps more importantly, these deposits will be of considerable interest as new computer memory planes and/or for a variety of microwave applications.

This laboratory has done considerable work on the CVD growth of epitaxial ferrites (Ref 4 thru 9) and garnets (Ref 11, 12).

Objective

It is the objective of the present contract to extend the CVD technology to the growth of epitaxial lithium ferrite films. They will be characterized with respect to crystal, electrical, and magnetic properties which will be of interest for memory and microwave applications.

Introduction to CVD of Metal Oxides

The reaction used for the CVD growth of a single crystal metal oxide may be represented as:

$$MX_{2(g)} + H_2O_{(g)} \xrightarrow[\Delta]{\text{seed}} MO_{(s)} + 2HX_{(g)} \qquad (1)$$

or

$$MX_{2(g)} + \frac{1}{2} O_{2(g)} \xrightarrow[\Delta]{\text{seed}} MO_{(s)} + X_{2(g)} \quad (2)$$

or a combination of 1 and 2. M represents the metal and X = Cl, Br, or I. To deposit a single crystal film one must have a single crystal seed or substrate; the substrate can be the same material as the deposit but does not have to be. For a more complex oxide such as manganese ferrite the deposition reaction may be written:

$$MnX_{2(g)} + 2FeX_{2(g)} + 3H_2O_{(g)} + \frac{1}{2} O_{2(g)} \xrightarrow[\Delta]{\text{seed}} MnFe_2O_{4(s)} + 6HX_{(g)} \quad (3)$$

For lithium ferrite the reaction may be written:

$$LiX_{(g)} + 5FeX_{2(g)} + \frac{11}{2} H_2O_{(g)} + \frac{5}{4} O_{2(g)} \xrightarrow[\Delta]{\text{seed}} LiFe_5O_{8(s)} + 11\ HX_{(g)} \quad (4)$$

The first work on the ferrites was begun in this laboratory in 1961. Epitaxial deposits of Fe_3O_4, $MnFe_2O_4$, $NiFe_2O_4$, $CoFe_2O_4$, and solid solutions of these compounds were grown on magnesium oxide (MgO) substrate crystals (Ref 4). The antiferromagnetic compounds NiO, CoO, FeO, MnO, $Ni_xCo_{1-x}O$ and $Mn_xFe_{1-x}O$ were also grown. Cech and Alessandrini (Ref. 13) had previously grown epitaxial deposits of FeO, CoO, and NiO. Takei and Takasu independently grew epitaxial ferrites by the same technique. A Russian team recently reported on switching properties of manganese ferrite films made by the same technique. (Ref 16). The work in this laboratory has progressed to the point where smooth, high quality ferrite films of controlled composition are grown routinely. These films are being characterized and developed as memory planes. The encapsulation of polycrystalline conductors in single-crystal ferrite (Ref 6) and the determination of the encapsulation mechanism (Ref 7) have been reported. In addition reports have been made on domain configurations and domain wall motion (Ref 7, 8, 9).

Several other single-crystal metal oxides have been grown by the CVD technique, including sapphire (Ref 14), SnO_2 (Ref 17), and ZnO (Ref 18, 19). In addition, the related process of closed-tube chemical transport has been used to grow Fe_2O_3 (Ref 20), Fe_3O_4 (Ref 21), ferrites (Ref 22, 23), and NiO (Ref 24). Finally, Robinson, et al (Ref 25), re-examined the deposition of FeO, NiO, CoO, Co_3O_4, and Fe_3O_4, but their conclusions with respect to the growth mechanisms are premature.

Acknowledgments

The authors would like to acknowledge G. R. Pulliam and J. L. Archer for major direction and efforts early in the program; J. P. McCloskey for the chemical analysis work; P. J. Besser and F. A. Pizzarello for suggestions and discussions on magnetic studies and applications; C. A. Newkirk and J. Haworth for preliminary magnetic measurements; E. F. Grubb for seed polishing; L. A. Moudy and E. R. Goldman for X-ray analyses; C. W. Laakso for the electron microprobe analyses; and W. G. Lynch for the synthesis of $FeCl_2$.

EXPERIMENTAL

Substrates

Magnesium oxide (MgO) crystals from Muscleshoals Electrochemical Corporation, Tuscumbia, Alabama, are presently being used for substrates in this program. These crystals generally have a bulk dislocation density near $1 \times 10^5 cm^{-2}$. The surface preparation depends on the particular deposition experiment but, in general, is designed so the surface dislocation density is not significantly greater than the bulk density (Ref 15). For much of the early work it was sufficient to use fresh cleaved {100} surfaces. These surfaces have large areas with the minimum $10^5 cm^{-2}$ dislocation count, but the count is higher (probably 10^6 - 10^8) in the immediate area where the seed is cleaved. In addition there are several cleavage steps across the face of the seed. At this stage of the work, the seeds are polished {100}'s and {110}'s. First they are mechanically polished on a Syntron machine using fine alumina grits so as not to generate deep damage into the MgO crystals. The {100}'s are checked with a dislocation etch (Ref 26) (5 parts saturated NH_4Cl, 1 part H_2SO_4, 1 part water) to make sure the surface is near the $10^5 cm^{-2}$ dislocation count. They are then repolished with fine alumina for a short time to remove the surface material affected by the etch. Finally they are chemically polished in 100 C phosphoric acid for one minute, and then rinsed in HCl, water, and methanol. The {110} surfaces are chemically polished in 165 C phosphoric acid for 1 minute and 45 seconds. They are checked with an etchant (of 9 parts conc. HNO_3, 10 parts H_2O at 90-100 C for 15 seconds) which appears to be a dislocation etchant, though this has not been rigorously proven.

Source Materials

Source materials for the epitaxial ferrite depositions have been limited to the anhydrous metal halides.

Both anhydrous ferrous bromide, $FeBr_2$, and $FeCl_2$, have been investigated as the iron source material. Precautions are necessary to prevent hydrolysis products which would result from the action of the moisture in the air on these hygroscopic salts. The hydrolysis products would seriously affect the vapor pressure and, hence, the transport rate of the $FeBr_2$ or $FeCl_2$. Experience has shown that reaction reproducibility with these materials is best using in-house synthesized material to achieve total control and history of the material preparation and handling. They are prepared by direct reaction of iron wire with the HBr or HCl gas at temperatures slightly above the melting point of the $FeBr_2$ or $FeCl_2$. The vertical fused silica reactor is designed so the molten $FeBr_2$ or $FeCl_2$ drips into a collecting crucible, thus leaving the metal exposed continually to the HX gas (Ref 27). A normal batch weighs from 250-350 grams and is in chunk form. This is desirable, since a minimum surface area is exposed to the air when the batch is unloaded. The anhydrous $FeBr_2$ and $FeCl_2$ are then stored in evacuated containers and are exposed to the air only briefly when they are transferred to the reactor.

Two lithium source materials have been used thus far, they are anhydrous lithium bromide (LiBr) and anhydrous lithium iodide (LiI).

The LiBr was from two sources:

1. Matheson-Coleman-Bell anhydrous LiBr sublimed in a molybdenum train in an evacuated fused-silica chamber.

2. Anderson Labs anhydrous LiBr of purity for fused salt applications. Thus we would expect it to be quite free of water or hydrolysis products. Its visual appearance indicated that it was very good material.

The LiI was commercial material, which was supposed to be anhydrous but which varied from nearly anhydrous to completely hydrated (from one to three waters of hydration) from bottle to bottle. To achieve uniformity, all material is routinely vacuum dried at approximately 450 C for several hours. This should give a product of approximately 98.9 percent anhydrous LiI with approximately 0.1 percent LiOH and some insoluble silicates (Ref 28). Its melting point was determined by a cooling curve technique to be 470 C. This compared to the best reported value of 469 C (Ref 29).

Depositions

Reactor design. - The deposition reactor is T-shaped (Figure 1) (Ref 5-8). The T is made of 57-mm OD fused-silica tubing with a 4-ft-long horizontal chamber and 3-ft-long vertical chamber. Because the fused-silica is quite susceptible to attack from the lithium halide vapors, a mullite liner is used in the most vulnerable region of the horizontal chamber. Earlier in the work, a complete mullite T was fabricated inside the fused silica T, but this was not always structurally sound. A fused silica liner is used in the vertical section. The remaining exposed reactor walls near the T-junction are slowly attacked (see the discussion under Results for possible Si contamination in the deposits).

Reactor operation. - In order to generate vapors of FeX_2 and LiX in the desired ratio, each source material is heated in a separate temperature zone of the reactor's vertical chamber. The crucible for FeX_2 is made of fused silica and for LiX is made of platinum. In a typical run using $FeCl_2$ and LiI, dry helium is introduced into the bottom of the vertical chamber at 21 ft^3/hr to transport the $FeCl_2$ and LiI vapors into the reaction zone. An additional 2 ft^3/hr of helium flows directly into the crucible holding the LiI to sweep the dense vapors into the gas stream. Helium, 2 ft^3/hr, is bubbled through water at room temperature and then, along with oxygen at 3.4 ft^3/hr is injected into the horizontal chamber. The reaction-deposition zone is in the horizontal chamber just downstream from the T-junction. The seeds are placed on a fused-silica holder in the horizontal chamber until the reaction conditions have been established; then they are carefully pulled into the deposition zone. A substrate holder cooled by swift flowing gas is used for experiments in which it is desired to have the seeds at a lower temperature than the rest of the reaction region.

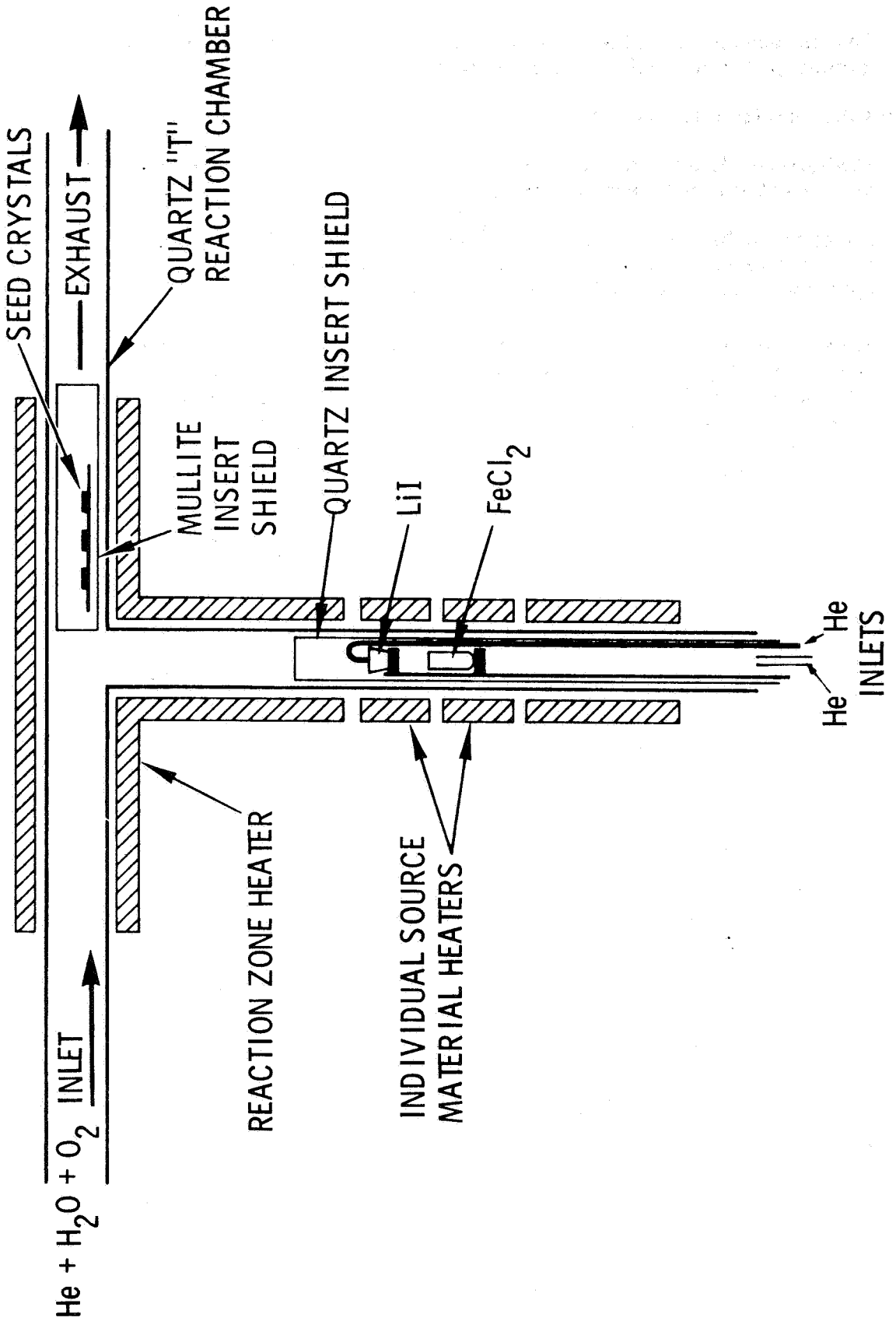

Figure 1. The T Reactor for Ferrite Deposition

Evaluation of LiX source materials. - The reactions

$$2LiX_{(g)} + H_2O_{(g)} \longrightarrow Li_2O_{(s)} + 2HX_{(g)} \quad (5)$$

and

$$2LiX_{(g)} + \frac{1}{2} O_{2(g)} \longrightarrow Li_2O_{(s)} + X_{2(g)} \quad (6)$$

were investigated to evaluate LiBr and LiI for preparation and handling problems, relative reactivities, transport conditions, reproducible behavior, etc.

Neither the MCB-LiBr nor the Anderson Labs - LiBr would react in the vapor phase under the highest oxidizing conditions that could be achieved conveniently in the T-reactor:

Vertical gas flow	He	= 10 ft^3/hr
Gas injected directly into LiBr cup to sweep out LiBr vapors	He	= 5 ft^3/hr
Horizontal gas flow	wet O_2	= 25 ft^3/hr
	He	= 2 ft^3/hr
LiBr transport rate	Up to 20 gm/hr	
Deposition zone temperature	950 - 1000 C	

The LiI vapors did react, especially under relatively high O_2 flow conditions. Typical conditions were:

Vertical gas flow	He	= 6 ft^3/hr
Gas injected directly into LiI cup to sweep out LiI vapors	He	= 11 ft^3/hr
Horizontal gas flow	wet He	= 3.5 ft^3/hr
	O_2	= 3.5 ft^3/hr
LiI transport rate	~20 gms/hr	
Seed temperature	890 C	

Mixed Fe-LiO depositions. - The most promising results have been obtained using $FeCl_2$ as the iron source material and LiI as the lithium source material for reasons

which will be discussed in the Results section of this report. Typical deposition conditions for the $FeCl_2$-LiI combination are as follows:

Vertical gas glow	He	= 21 ft^3/hr
Gas injected directly into LiI cup	He	= 2 ft^3/hr
Horizontal gas flow	wet He	= 2 ft^3/hr
	O_2	= 4 ft^3/hr
$FeCl_2$ transport rate	5.2 gms/hr	
LiI transport rate	5.4 gms/hr	
Seed temperature	840 - 890 C	

See the Results section for a discussion of the present understanding of the identity and nature of the products and the present key to understanding and reproducing the depositions.

Characterization

Characterization thus far has been limited to chemical analysis of the deposits, and determining if significant quantities of impurity elements are present. Lithium has too low an atomic number to permit simple X-ray fluorescence detection or electron microprobe detection. Its presence can be determined only by chemical or spectrographic analysis. Careful X-ray powder patterns could differentiate between lithium ferrite with a_O = 8.33 Å and Fe_3O_4 with a_O = 8.39 Å, but the possible presence of magnesium ferrite (by reaction with the substrate MgO) with a_O = 8.36 Å would make assignment by this technique somewhat questionable, especially if there were some solid solution.

Chemical analysis. - The film was dissolved from the magnesium oxide crystal by warming with a few milliliters of 6N HCl until the dark deposit was clearly removed. About 10 minutes dissolution time was required. The 6N HCl solution was passed through a small anion exchange column (chloride form) and then eluted with 6N HCl. The iron remained on the column, with the eluate containing all of the lithium and any magnesium that may have been dissolved. The iron was desorbed from the anion column with 1.0 N HCl and determined colorimetrically using Bathophenanthroline for color development.

The eluate containing the lithium and magnesium was evaporated to dryness removing excess acid, and the residue was dissolved in a few milliliters of distilled water. The lithium and magnesium were then absorbed on top of a small cation exchange column (hydrogen form). Desorption of the lithium from the column with 1.0 N HCl served to separate the lithium from the magnesium. The lithium was determined colorimetrically in the 1.0 N HCl eluate, with "Thoron" reagent.

The deposits are examined by electron microprobe for possible significant impurity elements from unreacted LiI or from attack of reactor materials. However, in most of the deposits, no I, Si, or Al has been detected. In a few deposits I was detected; these were always under preparation conditions where simple LiI condensation could explain the presence of I. Subsequent runs were made at higher substrate temperatures to avoid LiI condensation. Occasionally Si has been detected but there has been no consistent pattern as to when it will be present.

X-ray and electron microscope. - A full array of X-ray and related techniques are used to help characterize the deposits with respect to single crystallinity, orientation, and identity. Differentiation between stoichiometric lithium ferrite and other possible similar products is very difficult by these techniques.

Magnetic measurements. - At present no significant magnetic measurements have been made on the deposits. Magnetic measurements are now beginning, and details will be given in later reports.

RESULTS AND DISCUSSION

Substrates

Generally, good quality epitaxial deposits of metal oxides by the CVD technique have only been achieved under the following substrate-deposit conditions:

1. There is some reasonable lattice match between part or all of the occupied lattice sites in the substrate surface and some likely orientation of the desired deposit (Ref 8).

2. The substrate orientation is compatible with deposit growth peculiarities such as preferred growth directions.

3. The substrate is inert with respect to side or competing reactions.

4. There is a reasonable fit of thermal expansion coefficients between the substrate and deposit.

5. The substrate surface has been fresh cleaved or chemically polished so as to present a minimum dislocation count surface.

The substrate for the lithium ferrite depositions, as for the other ferrite depositions, is magnesium oxide (MgO). The lattice constants of the spinel structured ferrites are around 8.40 Å, while the value for the NaCl structured MgO is 4.21 Å. Although the lattice constants of the ferrites are twice the MgO, in both structures the oxygen ions are cubic close-packed. The oxygen-oxygen distances are virtually identical in the two systems so epitaxial growth of the ferrites on MgO requires that only the metal ions adopt different sites in the overgrowth. The MgO crystals are reasonably inexpensive, have convenient $\{100\}$ cleavage planes for easy referencing, and have coefficients of expansion in the range of the ferrites. Techniques have been worked out for chemically polishing various MgO orientations so that good $\{100\}$'s, and good $\{110\}$'s, and fair $\{111\}$'s can be prepared. There are some questions as to how inert the MgO is and what is the best orientation for the lithium ferrite deposition (discussed in the section on Depositions and Characterization).

Source Materials

The choice of ferrous chloride, $FeCl_2$, as the iron source material, and lithium iodide, LiI, as the lithium source materials is mainly due to the chemical thermodynamics involved in the deposition reaction (discussed in the section on Depositions and Characterization).

Initially, ferrous bromide and lithium bromide were apparently used successfully to deposit films with Fe:Li ratios near that required for lithium ferrite. This work was never reproduced. Subsequent experiments using LiBr failed to give any Li-containing deposit. In reviewing the original successful depositions, it was noted

that they occurred in a reactor tube that had been used for sometime for other ferrite depositions. This suggests two possibilities:

1. There was a certain buildup of ferrite on the reactor walls near the T-junction. The lithium bromide vapors may have reacted with the ferrite giving a volatile, complex compound containing lithium, iron, oxygen, and bromine. In the deposition zone the added H_2O and O_2 could have oxidized this complex to form the solid lithium ferrite.

2. It is known that the lithium halide vapors react to varying degrees with the reactor material, e.g., with fused silica or mullite. It may be that in the successful runs, the reactor walls had been conditioned by poisoning or coating. This would prevent or minimize the lithium halide from reacting with the reactor walls and permit the lithium halide to be more readily available for the desired oxidation reaction. There is evidence that this type of thing occurs in garnet depositions.

The possibilities are in the realm of speculation and should not be interpreted as proven explanations. There remains the possibility that the lithium ferrite did form according to the proposed reaction,

$$LiBr_{(g)} + 5FeBr_{2(g)} + \frac{11}{2} H_2O_{(g)} + \frac{5}{4} O_{2(g)} \xrightarrow[\Delta]{\text{seed}} LiFe_5O_{8(s)} + 11HBr_{(g)} \qquad (7)$$

but that some controlling activating phenomenon involving the LiBr could not be reproduced. It did not appear to be a simple matter of using higher purity material. This is reminiscent of some early work on the manganese ferrite depositions in which different batches of high purity manganese bromide reacted at widely different rates. The cause for this difference in reactivity was obscure and was never determined, but reproducibility was obtained by using in-house synthesized material and standardizing the preparation procedure.

Depositions and Characterization

Reactor problems. - The lithium halide vapors react to varying degrees with usual reactor materials such as fused silica, mullite, or alumina. The lithium bronide was very bad in this respect, but even the lithium iodide attacks the reactor material to a certain extent. Because of this there are two changes in the lithium ferrite reactor compared to the other ferrite T-reactors. First, a mullite liner is used in the deposition zone to protect the fused silica reactor walls. Second, there is less premixing of the metal halide vapors in the vertical chamber because of the need for much simpler design of the pre-mix tube. In other ferrite depositions this pre-mix tube, made of fused silica, has a very restricted opening at the top plus a baffle. This arrangement permits the metal halides to mix before they meet the oxidizing gases, and it helps give a symmetrical flow pattern in the reaction zone. In the lithium ferrite reactor, both the restriction and the baffle have had to be removed because the fused silica was severely attacked by the lithium halide vapors. The remnant of the pre-mix tube serves little purpose other than to channel the LiI vapors into the center

of the vertical chamber. It apparently does this fairly successfully since the upper reactor walls are attacked only slowly. However, the flow patterns are not always as symmetrical as desired, so some sort of device may have to be worked out to improve them.

Reactivity considerations. - Once a choice of substrates and source materials has been made, the optimum conditions for epitaxial depositions must be determined. The primary consideration is to find growth conditions that favor a reaction at the surface, i.e., a heterogeneous reaction, rather than a homogeneous gas phase reaction. The surface reaction leads to single crystal growth whereas the gas phase reaction is likely to give a polycrystalline, even powdery, deposit. Certainly the substrate plays some role in this although its exact nature is not understood. For example, instances have been reported (Ref 13, 25) in which growth was apparently limited to MgO substrate surfaces. It has been shown (Ref 6) that ferrite growth can be continued on a ferrite surface under conditions where an adjacent gold conductor surface experiences no nucleations or growth of ferrite. However, reactivity of the source materials is very important in determining whether the reaction will be limited to the surface or will occur readily in the gas phase. Thermodynamic calculations will indicate whether a given source material should be very reactive, moderately reactive, or essentially nonreactive, but the available data (free energies of formation, etc.) does not permit more accurate predictions. Of course, the actual chemical kinetics of the reaction can hinder or prevent a supposedly feasible reaction.

It is also possible to slow down a given reaction by adding $HX_{(g)}$ to the reaction chamber. This is very necessary for the depositions of yttrium iron garnet, $Y_3Fe_5O_{12}$, because the YCl_3 vapors are very reactive with respect to oxidation (Ref 11, 12). In the ferrite growth this has not been necessary because the source materials used are only moderately reactive; the ferrite deposition rate can be adequately controlled merely by controlling the concentrations of the source materials and oxidizing gases in the reaction zone.

In the lithium ferrite depositions the problem is just the reverse - the lithium halides are almost nonreactive with respect to oxidation under reasonable deposition conditions. Thermodynamic calculations have been made to help predict the reactivity of the lithium halide source materials. The approach was to calculate the free energy of reaction (ΔG) for each source material separately. Thus for lithium bromide the ΔG_{rx} for the reactions

$$2LiBr_{(g)} + H_2O_{(g)} \rightarrow Li_2O_{(s)} + 2HBr_{(g)} \quad (8)$$

and

$$2LiBr_{(g)} + \frac{1}{2} O_{2(g)} \rightarrow Li_2O_{(s)} + Br_{2(g)} \quad (9)$$

are of interest over the temperature range of approximately 700 C to 1200 C.

The ΔG_{rx} is calculated from the known or estimated free energies of formation (ΔG_{form}) of the products and reactants involved in the reactions 8 and 9. Using reaction 8 as an example,

$$\Delta G_{rx} = 2\Delta G_{form\ HBr_{(g)}} + \Delta G_{form\ Li_2O_{(s)}} - 2\Delta G_{form_{LiBr_{(g)}}} -$$

$$\Delta G_{form\ H_2O_{(g)}}$$

at the temperature of interest. The ΔG_{form} values are listed in Table I. However the

$$\Delta G_{form\ LiBr_{(g)}}$$

for temperatures below 1500 K must be obtained by adding $\Delta G_{vaporization}$ to the ΔG_{form} value for the listed condensed phase (liquid or solid). The ΔG_{vap} is given for 1000 K only. For other temperatures estimates must be made. The estimating method used was to calculate

$\Delta G_{vap} = \Delta H_{vap} - T\Delta S_{vap}$ and use $\Delta H_{vap} = 40.77$ kcal/mole and

$\Delta S_{vap} = 28.2$ cal/mole (Ref 30).

This assumes ΔH_{vap} is constant over the temperature range of the calculations.

The calculations indicate $\Delta G_{reaction\ 8} = +14$ kcal/mole Li_2O at 1000 K and +30 kcal/mole Li_2O at 1300 K, and $\Delta G_{reaction\ 9} = -4$ kcal/mole Li_2O at 1000 K and +18 kcal/mole Li_2O at 1300 K. A large positive ΔG of course indicates that the reaction is thermodynamically not feasible. The small negative ΔG for reaction 9 at 1000 K indicates that, at least thermodynamically, there is a small driving force for this reaction at this temperature. Any added driving force for the formation of lithium ferrite cannot be calculated because there is no data known on the free energy of formation of the lithium ferrite. If the ΔG_{form} of the lithium ferrite is not great, then the oxidation of LiBr is limited to reaction 9 at temperatures (approximately 1000 K) where the reaction is complicated by condensation of some of the LiBr vapors. Finally, possibility of competing products such as LiOBr is unknown.

Similar calculations with lithium iodide as the lithium source material are more favorable. The reactions are:

$$2LiI_{(g)} + H_2O_{(g)} \rightarrow Li_2O_{(s)} + 2HI_{(g)} \quad (10)$$

$$2LiI_{(g)} + \frac{1}{2} O_{2(g)} \rightarrow Li_2O_{(s)} + I_{2(g)} \quad (11)$$

TABLE I
THERMODYNAMIC DATA FOR ΔG_{rx} CALCULATIONS

Species	Free Energy of Formation, (a) $-\Delta G_{form}$			Free Energy of Vaporization, (b)	Probable Accuracy	
	500°K	1000°K	1500°K	ΔG_{vap}, 1000°K		
LiBr	$77.4_{(s)}$	$67.8_{(1)}$	$61.1_{(1)}$	13.9	±2	
LiI	$63.3_{(s)}$	$54.4_{(1)}$	$48.2_{(g)}$	13.1	±2	s = solid
$FeCl_2$	$66.8_{(s)}$	$53.2_{(1)}$	$50.1_{(g)}$	6.8	±0.4	
$FeBr_2$	$50.9_{(s)}$	$38.4_{(1)}$	$30.4_{(g)}$	4	±1	
$FeCl_{3(g)}$	72	63	52		±1	1 = liquid
$FeBr_3(g)$	51				±4	
$Li_2O_{(s)}$	127.6	111.7			±1	
$Fe_2O_{3(s)}$	166	133	105		±5	g = gas
$H_2O_{(g)}$	52.4	46.0	39.3		±0.3	
$HCl_{(g)}$	23.0	23.9	24.6		±0.3	
$HBr_{(g)}$	14.2	15.1	15.9		±0.3	
$HI_{(g)}$	2.3	3.2	4.1		±0.3	

Reference: (a) C. J. Smithells, Metals Reference Book, Volume II, Butterworths, 1962.

(b) L. Brewer, L. A. Bromley, P. W. Gilles, N. F. Lofgren, "The Thermodynamic Properties of the Halides," p. 76, Chemistry and Metallurgy of Miscellaneous Materials, edited by L. L. Quill, Mc-Graw Hill Book Company, New York, 1950.

For reaction 10, $\Delta G_{reaction}$ = -10 kcal/mole Li_2O at 1000 K and +30 kcal/mole at 1300 K but for reaction 11, $\Delta G_{reaction}$ = -29 kcal/mole Li_2O at 1000 K and -5 kcal/mole Li_2O at 1300 K. Thus reaction 11 should be favorable over a considerable temperature range. This does not take into account possible complications due to the kinetics involved or competing products. Finally the calculations can only serve as a general guideline because of several unknowns such as free energy of formation of the lithium ferrite, possible competing products, and certain estimates and approximations in the calculated free energies of formation of the vapor state of the LiBr and LiI. So ultimately the experiments must be done to check the calculations. This was done. Depositions of Li_2O (on MgO) were attempted using anhydrous LiBr and anhydrous LiI as the lithium source materials.

The results were in qualitative agreement with the calculations. The LiBr could not be made to react to give Li_2O under even the most oxidizing conditions whereas the LiI did in fact give Li_2O films (apparently) at 800 C and high O_2 concentrations. The films were hygroscopic and did not contain any I from unreacted LiI, or Si or Al from reactor material contamination. On $\{100\}$ MgO, the films were discontinuous in the form of crystallites with edges aligned along the $\langle 100 \rangle$ directions (Figure 2). The form of the crystallites suggested that growth in the $\langle 100 \rangle$ direction was very fast so that $\{100\}$ faces quickly grew out of existence leaving faces of higher index (e.g. 100's and 111's). A couple runs were made using $\{111\}$ MgO seeds and continuous films were readily obtained (Figure 3).

X-ray Laues indicated ordered polycrystalline deposits with the lattice constant close to the 4.611 A for LiO. There is an apparent thermal expansion coefficient mismatch between the Li_2O and MgO causing the observed cleaving of the deposit. There was no effort to explore this system any further since the main goal was simply to evaluate the reactivity characteristics of the LiBr and LiI.

However, under otherwise identical conditions which gave Li_2O deposits when only LiI is used, when the iron halide was added to the system there was a marked drop in the reactivity of the LiI. This was especially so when $FeBr_2$ was the iron halide used; only powdery iron oxide deposits were obtained. Among several possible reasons for this behavior, the most reasonable one appeared to be that the more reactive $FeBr_2$ was readily reactive with the oxygen, thus lowering activity of the oxygen below a level that would permit the LiI to react. This reasoning is qualitatively consistent with thermodynamic predictions. To test this as the most reasonable hypothesis, $FeCl_2$ was tried as the iron source material, since calculations showed that, thermodynamically, it should be less reactive. Whether, in fact, the difference in reactivity would be significant could not be predicted. For the reaction

$$2FeCl_{2(g)} + \frac{3}{2} O_{2(g)} \rightarrow Fe_2O_{3(s)} + 2Cl_{2(g)} \qquad (12)$$

the calculated free energy of reaction ΔG_{rx} is -41 kcal/mole at 1000 K and -5 kcal/mole at 1500 K. For the reaction

$$2\ FeBr_{2(g)} + \frac{3}{2} O_{2(g)} \rightarrow Fe_2O_{3(s)} + 2Br_{2(g)},$$

the calculated ΔG_{rx} is -65 kcal/mole at 1000 K and -45 kcal/mole at 1500 K. Unfortunately, it is preferable to perform the depositions at 1175 K where, even

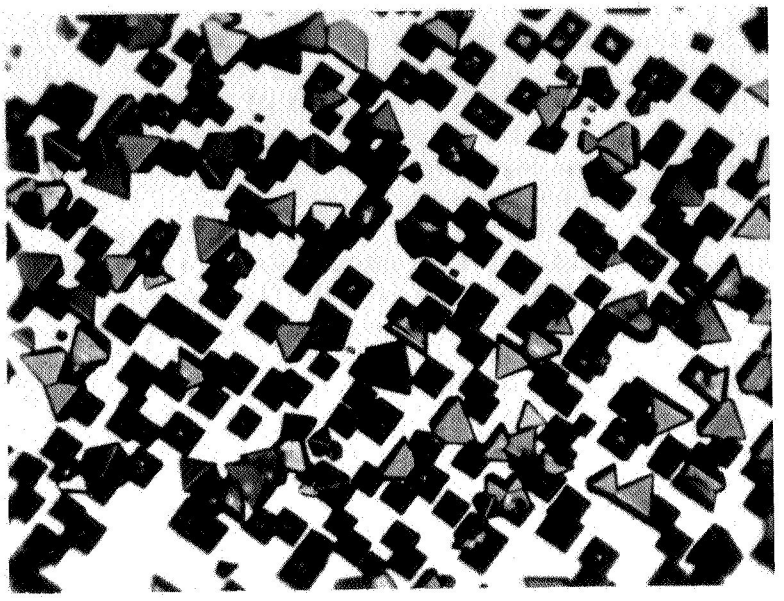

Figure 2. Ordered Li_2O Crystallites on a {100} MgO Substrate (360X)

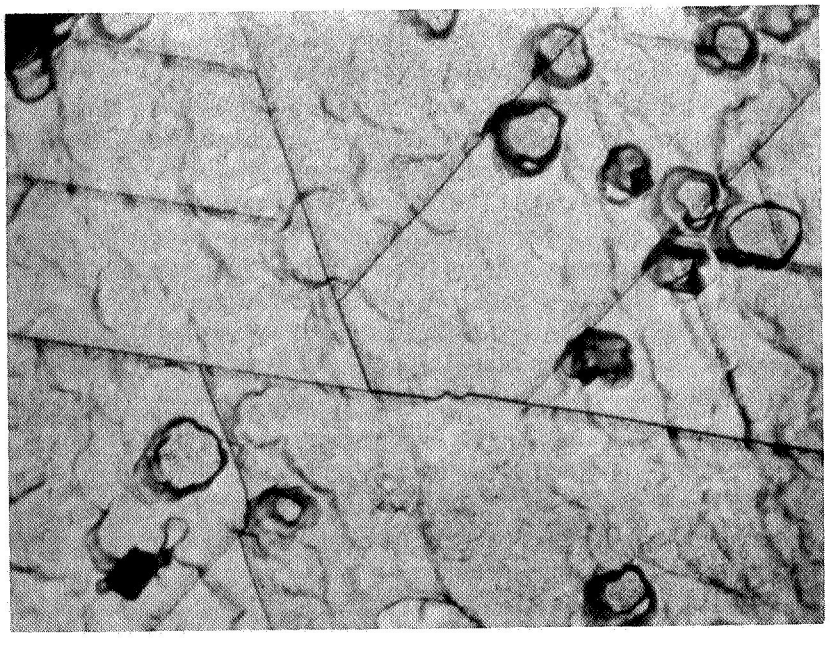

Figure 3. Continuous Film of Li_2O on a {111} MgO Substrate (360X)

with $FeCl_2$, there would still be an appreciable driving force for this reaction (interpolating the above data gives -58 kcal/mole for $FeBr_2$ at 1175K and -28 kcal/mole for $FeCl_2$). However, the calculations are only approximate and do not reflect chemical kinetic factors so again the experiments must be performed. This was done and the results were encouraging. In several runs using LiI and $FeCl_2$ as source materials the effect of the $FeCl_2$ on LiI reactivity appeared to be less than the effect of the $FeBr_2$. There was still an effect but it was much less pronounced.

Results of lithium ferrite deposition experiments. - Having determined that the source materials $FeCl_2$ and LiI react to produce oxide deposits containing Fe and Li, there still remain somewhat imposing problems. First, the deposits must be identified. Second, a systematic program of deposition experiments must be established which will lead to the growth of good quality, single crystal lithium ferrite. Care must be taken to rigorously prove:

1. That the deposits are lithium ferrite, or
2. If the deposits are not lithium ferrite, that the products be identified and the growth parameters adjusted accordingly.

Decisions must be made as to what the best analytical methods are at a given point in the program. Since lithium has too low an atomic number to be detected by electron microprobe or X-ray fluorescence techniques, its presence can only be determined by a destructive chemical analysis. X-ray patterns do not clearly identify lithium ferrite as opposed to other possible products which have very similar structures. Magnetic measurements of such properties as saturation magnetization vs T, Curie temperature, and resonance line width, with supporting X-ray and chemical analysis data ultimately will be the most definitive way to identify the films.

In general, the deposits have been epitaxial, continuous, and magnetic. They range in appearance from opaque to translucent red to transparent reddish-tan and in thickness from $\sim 1\mu$ to $\sim 10\mu$. They have not been identified yet, but evidence for identification is being accumulated.

It is desirable to speculate first about the possible products that could be formed in the reactors and then to cite the present evidence.

Possible products include α-Fe_2O_3, γFe_2O_3, Fe_3O_4, $MgFe_2O_4$, $LiFe_5O_8$, $LiFeO_2$, and mixtures or solid solutions of two or more of these. Because of the greater reactivity of the $FeCl_2$ over the LiI, Li_2O is not expected as a product under normal concentrations of both source materials. Also there has been no evidence for partially oxidized intermediates such as oxyhalides or hydroxyhalides. Iodide has been detected in some deposits but only under low temperature seed conditions where simple condensation of the LiI could explain it. The presence of unusual products due to impurities or due to reactions with reactor materials is guarded against by electron microprobe and emission spectrograph analyses on selected samples.

The α-Fe_2O_3 would not grow epitaxially on $\{100\}$ MgO; it is normally observed as a fine powder or as a precipitated second phase with a major ferrite phase. And, of course, it would be only very weakly magnetic.

Takei (Ref 31) has reported the deposition of epitaxial γ-Fe_2O_3 on $\{100\}$ MgO by a CVD technique. γ-Fe_2O_3 was deposited at temperatures as high as 700 C.

Thicknesses were limited to 1μ. For thicknesses exceeding that value polycrystalline α-Fe_2O_3 appeared on the surface. γ-Fe_2O_3 may be stabilized at even higher temperatures by the presence of a small amount of lithium.

The Fe_3O_4 is known to grow epitaxially on MgO to produce an opaque film which peels away from the substrate because of the thermal expansion mismatch with the MgO. An appreciable amount of Fe_3O_4 is not expected to be formed under the present oxygen conditions. However, a small amount may appear in solid solution with other ferrite compositions.

The $MgFe_2O_4$ definitely could appear as a result of a reaction between the iron species present and the MgO substrate. Production of epitaxial $MgFe_2O_4$ on MgO by such a mechanism has been reported by Autonetics and by others (Ref 11, 32). The conditions were different than the present growth donditions but the possibility of $MgFe_2O_4$ exists and will have to be verified one way or the other.

The $LiFeO_2$ as such would not be magnetic, but it might be present in small amounts as a separate phase or in solid solution with the $LiFe_5O_8$; although the partial phase diagram (Ref 33) indicates little if any solid solution should exist.

It was arbitrarily decided to submit most of the early deposits for wet chemical analysis. The iron and lithium content was determined to establish the Fe:Li ratio in deposits from different zones in the reactors and to make sure there was any lithium at all in the deposits. It was predicted and verified that products with a high Fe:Li ratio would be formed first in the reactor. Deposits with successively lower Fe:Li ratios would be formed downstream. However, until these analyses were performed, it was not known what level of lithium to expect in each deposit zone.

Six of the deposits contained iron and lithium in a weight ratio very near the 40.3:1 required for stoichiometric $LiFe_5O_8$. These were always the very thin (~1μ) deposits. Most of the samples analyzed contained lithium at between one-third and one-half the amount required for stoichiometric $LiFe_5O_8$; thus the Fe:Li weight ratio varied from ~120:1 to ~90:1. For samples from the same run, the first deposits always had a higher Fe:Li ratio than deposits from zones further downstream. This zone-type behavior is common to CVD of ferrites and garnets in the T-reactors once reasonably compatible source materials and reaction conditions are found.

Present deposits, both those with the desired Fe:Li ratio and some of the low Li deposits, give very rough deposits on the {100} MgO seeds. However, when viewed across a cleaved edge (Figure 4), the lack of smoothness appears to be due to a pyramidal type growth in which the {100} planes rapidly grow out of existence leaving exposed higher indexed planes. Deposits on {110} planes are somewhat better but are still not smooth. The surfaces show an ordered, saw-tooth ridge-like structure (Figure 5) with the long dimension of the ridges parallel to the 100 direction in the substrate. Figures 6 through 8 show how this surface structure appears when viewed from the top and across different cleaved edges of the sample. The cleaved views of the {100}'s and {110}'s indicate that the deposits are single crystals, or at least start to grow as single crystals, but the surfaces are not smooth because of certain growth peculiarities. Both surfaces can be explained, at least partially, in terms of preferred growth directions. It appears that {111} substrates should be tried to obtain smooth deposits.

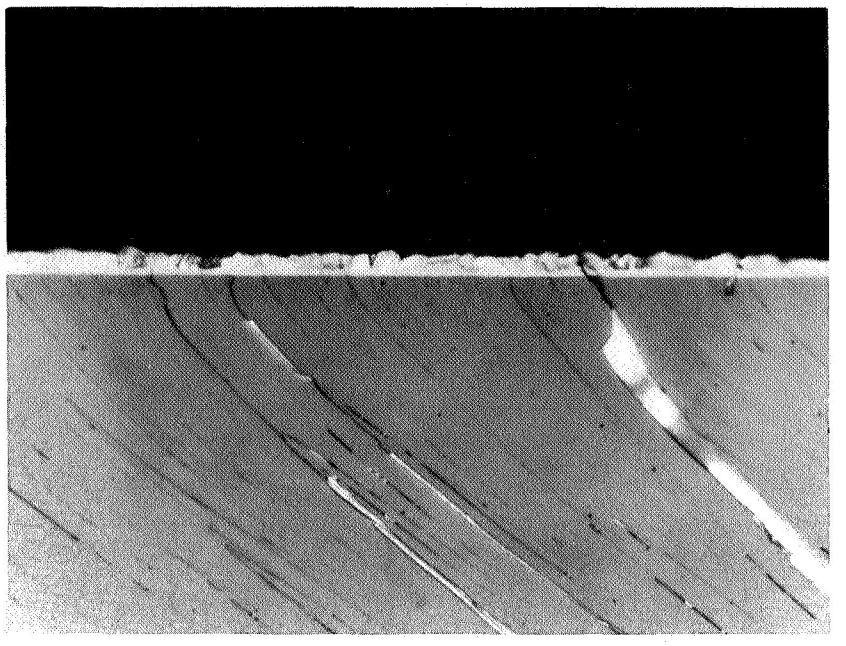

Figure 4. Cross Section of a Ferrite Deposit on a {100} MgO Substrate (360X)

The lower the lithium content, or the higher the Fe:Li ratio, the smoother are the {100} deposits. The change appears to be quite gradual. The first seed will have a fairly smooth deposit, the second deposit will be smooth at one edge and gradually get rough, and the following deposits will be rough. On the {100} deposits this roughness is due to tiny inverted square pyramids (Figure 9); these appear as dark areas using transmitted light (Figure 10).

In a few early, low-lithium {100} deposits, at the region of transition from opaque to red there was a second phase aligned in <110> directions (Figure 11).

In the translucent red, {100}, low-lithium deposits, large <110> type domains (Ref 8) were observed by the transmitted magneto-optic effect.

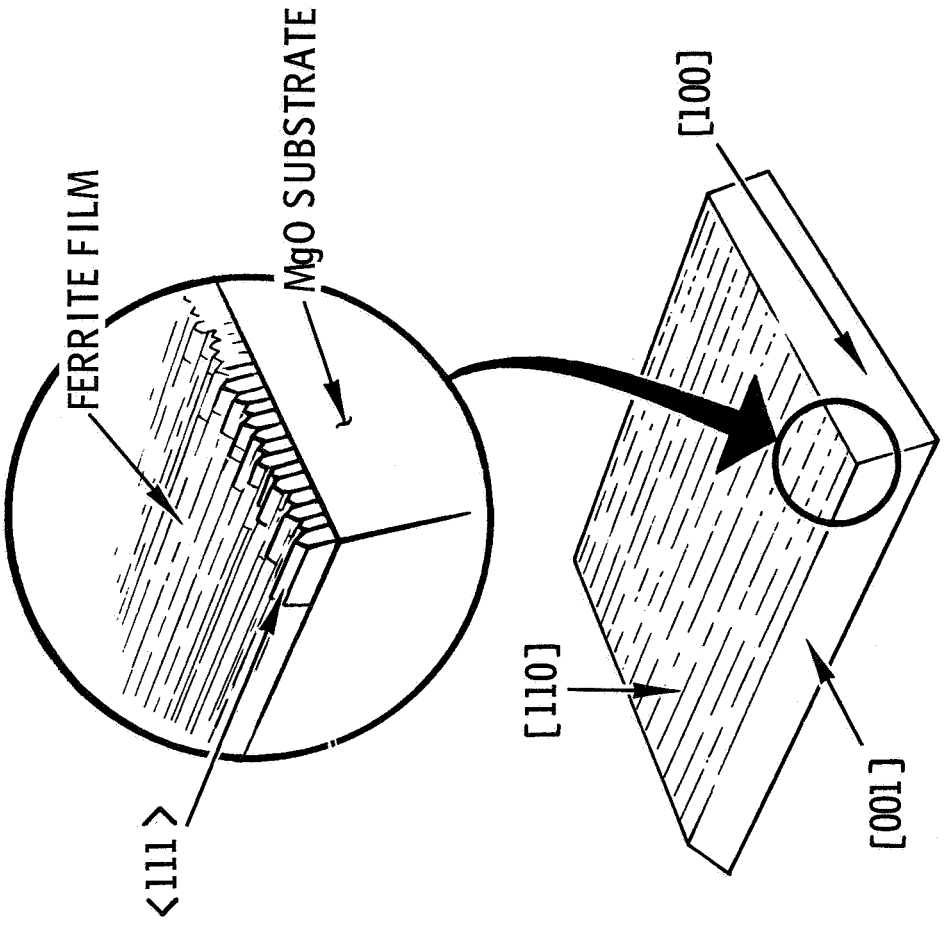

Figure 5. Drawing of a Typical Ferrite Deposit on a {110} Substrate

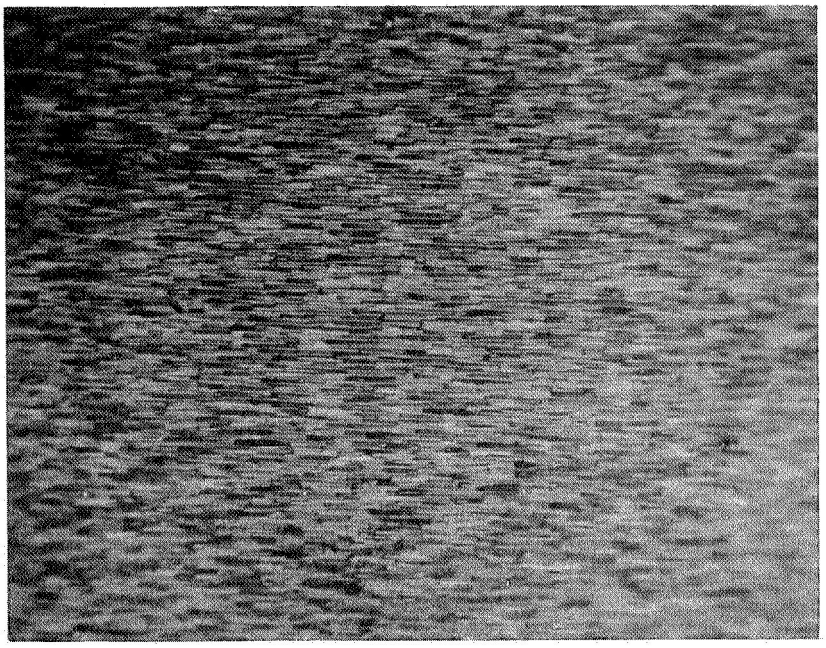

Figure 6. Top View of Ferrite Deposit on a {110} MgO Substrate (360X)

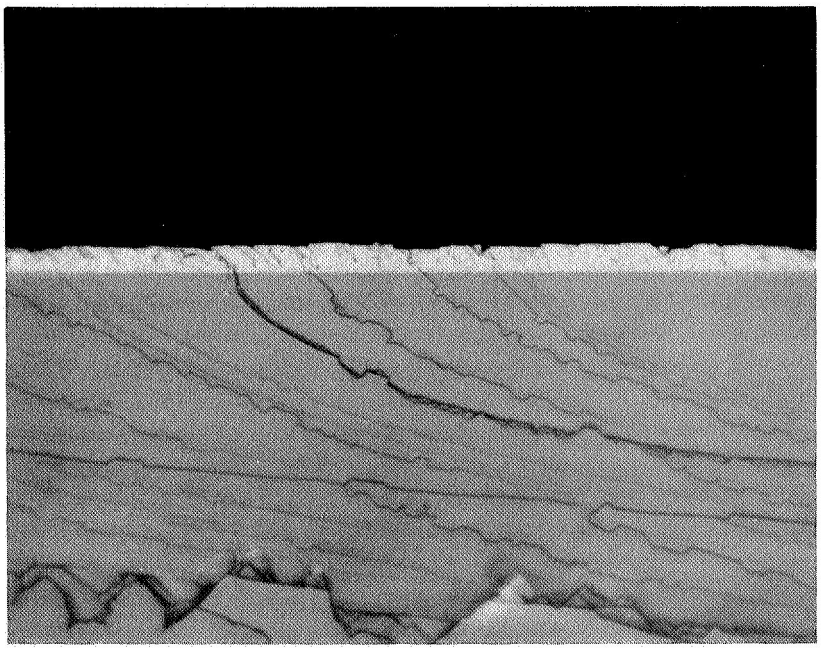

Figure 7. Cross Section of a Ferrite Deposit on (110) MgO Cleaved Along the (001) Plane. (360X)

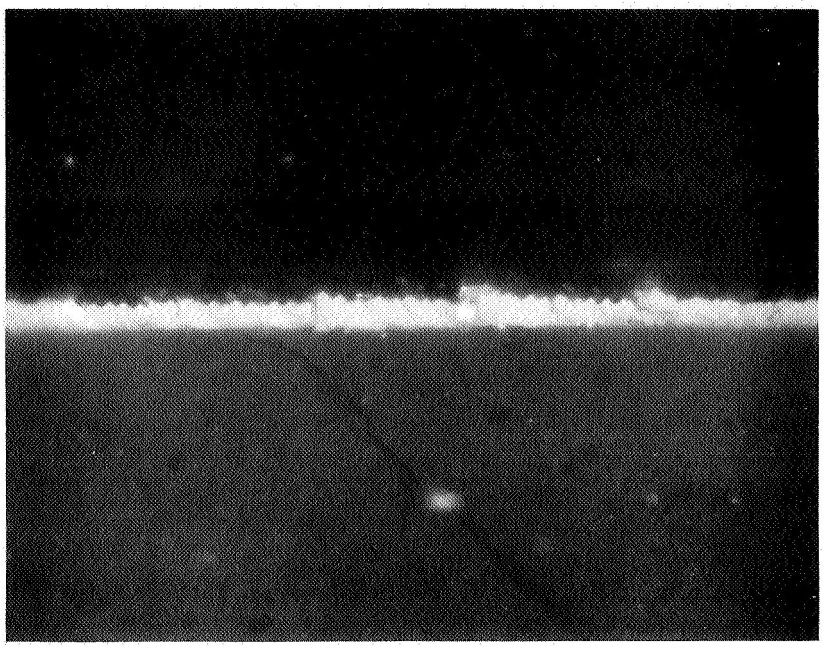

Figure 8. Cross Section of a Ferrite Deposit on (110) MgO Cleaved Along the (100) Plane. (1120X)

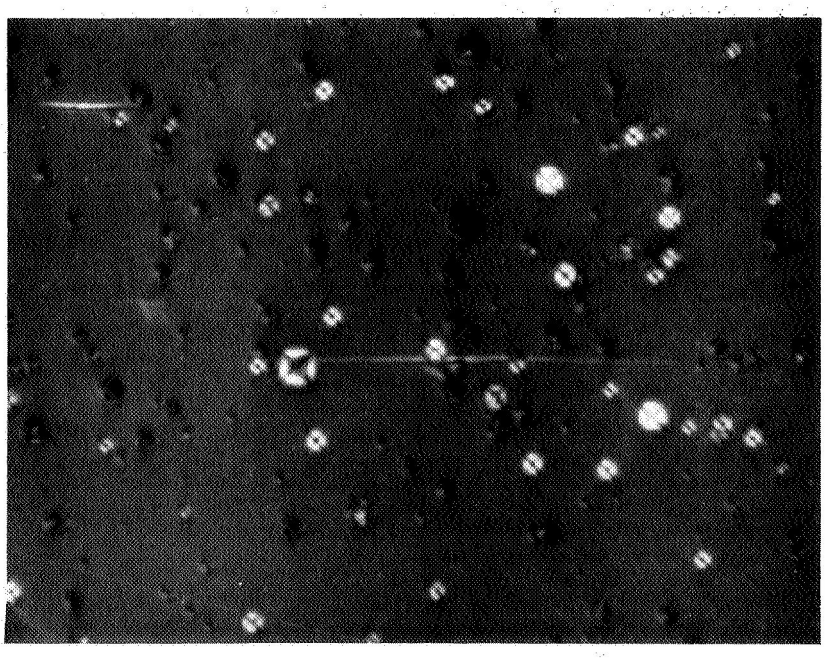

Figure 9. Surface of Ferrite Film Using Polarized Reflected Light (750X)

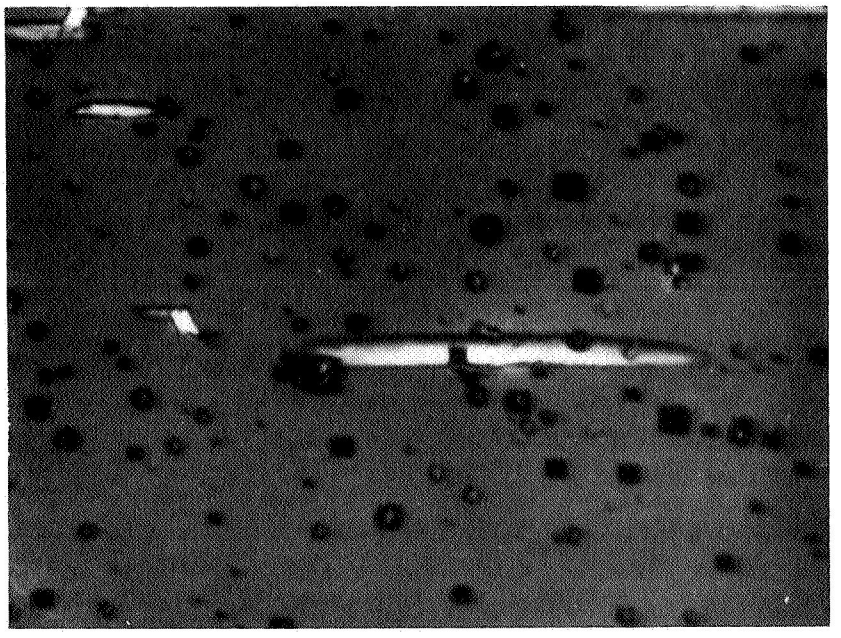

Figure 10. Same Area as Figure 9 Using Transmitted Light (750X)

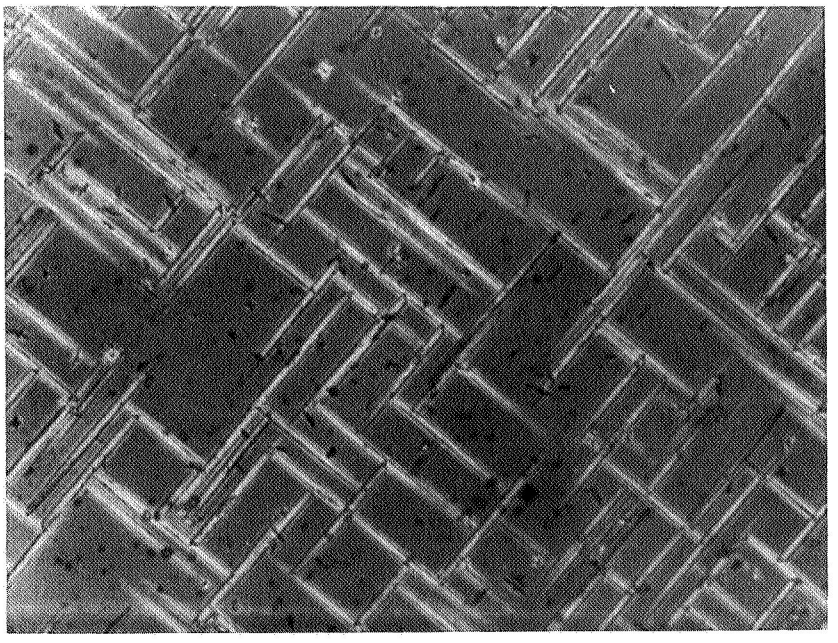

Figure 11. Second Phase (250X)

ANALYSIS OF PROGRAM

Interpretation, Speculation and Ultimate Objectives

Problem Areas. - There are three major problems associated with CVD growth of epitaxial lithium ferrite:

1. Lithium halides are considerably less reactive than the iron halides in the proposed deposition reactions.

2. Lithium halides react with the usual convenient reactor materials such as fused-silica, mullite and alumina.

3. Lithium cannot be detected by any nondestructive analytical technique.

Items 1 and 2 have been solved, at least in part. Iron trihalide might be considered as a further refinement in solving 1, but this presents other problems in preparation and in reactor design and control. It does not appear to be necessary at this time. Vigilance must be maintained against impurities in the deposits and other problems due to item 2. Item 3 is an unfortunate fact of life that slows down progress but does not prevent it altogether.

Another possible problem is that MgO may not be sufficiently inert with respect to competing side reactions. It may be impossible to obtain $LiFe_5O_8$ free from partial solid solution with $MgFe_2O_4$. However, now that the zone behavior has been established, other substrates could be used. This is not seen as an insoluble problem.

Areas of most significant progress. - Deposits of Li, Fe oxides are being produced with a fair degree of reproducibility and understanding. It seems likely that those deposits with analyzed Fe:Li weight ratios near 40.3:1 are the desired $LiFe_5O_8$. However, it is not yet possible to describe the deposits too rigorously in terms of stoichiometry, purity, state of ordering, extent of the $LiFe_5O_8$ zone, etc. These things will be determined by careful study of products from different zones. The emphasis in analysis methods is now shifting to magnetic measurements with X-ray and chemical analysis used more in supporting roles.

The early emphasis on chemical analysis paid off in giving at least a broad definition of the zone-type deposition behavior. Establishing this behavior is a positive step in this program. It gives some insight into the deposition process and it permits prediction and systematic experimental verification of effects due to changing the various parameters. Further experiments and characterization will, in turn, provide a more detailed definition of the nature of the deposits and the deposition process. It is not a primary goal of this program to identify and characterize the low-lithium deposits but some characterization will be necessary to understand the lithium ferrite deposition process.

In summary, the present results are very encouraging, and it is believed that good quality epitaxial $LiFe_5O_8$ will be attained and rigorously identified.

Future Work

Growth. - Presently the deposits with the desired Fe:Li ratio are rough and very thin and thus difficult to analyze. The roughness appears to be due to preferred growth directions and available data indicate more {111} substrate surfaces should be tried. These are now being prepared. To obtain thicker deposits, possible approaches are to:

1. Investigate effects of deposition temperature.
2. Investigate effects of varying concentrations of the reactants.
3. Investigate the vertical growth gradient in the reactors; i.e., determine the vertical nature of the deposit zones.
4. Investigate the gas flow characteristics to permit better mixing of the oxidizing agents with the lithium and iron source materials.
5. Investigate special reactor schemes such as a double T reactor or prereacted lithium source material.

Item 1 is now being investigated via application of a special substrate holder that permits local cooling in the reaction zone. Depending on the results of this study, it may or may not be necessary to try 4 and 5. Certainly 2 and 3 will have to be optimized sooner or later.

Characterization. - The emphasis in analysis methods is now shifting to magnetic measurements. Initial product identification will depend on M_S vs T, and Tc determinations with supporting X-ray and chemical analysis data. Static coercive force measurements will be utilized to check on reproducibility of deposits and the magnetic anisotropy of the sample. Resonance experiments will be used primarily to indicate crystal quality. Thus the major near-future goal of the magnetic measurements will be to identify the deposits. Once the deposits are identified, the goal will shift to characterizing them with respect to properties potentially useful for memory and microwave devices.

Possible device applications. - Some of the memory application concepts now being developed with the epitaxial $Mn_xNi_{1-x}Fe_2O_4$ films (Ref 7) should be applicable to epitaxial lithium ferrite. There are two major models of the epitaxial ferrite memory planes at this time - the encapsulated model and the miniature picture-frame model. It does not appear feasible at this time to achieve encapsulation of a conductor array in the lithium ferrite crystals. But the picture-frame model is certainly a possibility.

There are also distinct possibilities that epitaxial lithium ferrite will be very useful in new, miniaturized microwave devices. Garnet and ferrite films, both polycrystalline (Ref 34) and single crystal (Ref 35), are already being investigated in this area. However, considerable study of these materials is required to determine the advantages and disadvantages of the deposit-substrate combinations.

The crystal quality of crystals grown by CVD should be comparable to or better than crystals grown by more classical methods. Thus a room temperature resonance line width of 55 oersteds was measured on one of our epitaxial $MnFe_2O_4$ films. This compares to the best line widths reported for single crystals of this material. Epitaxial YIG films on YAG and on GdGaG have shown line widths of 1.1 - 1.5 oersteds. Epitaxial YIG on YIG has a linewidth of 0.6 oersteds. There is every reason to believe that epitaxial lithium ferrite can be achieved with linewidths as good as other single-crystal lithium ferrite, i.e., around 1 oersted. In particular, lithium ferrite looks extremely interesting in the magnetoelastic device area for transducers and/or delay media because of the combination of good magneto-elastic coupling and narrow resonance line width (Ref 36, 37).

It appears that the epitaxial lithium ferrite deposits will be transparent or, at least, translucent up to thicknesses of several microns. It will be of interest to compare their magneto-optic properties with other studies and proposed applications in the magneto-optic area.

Finally, the aforementioned temperature stability of Li ferrite along with the square hysteresis loop property make it potentially very promising for microwave latching applications if it can be fabricated with low dielectric losses (Ref 38).

REFERENCES

1. J. P. Remeika and R. L. Comstock, "Properties of Single-Crystal Lithium Ferrite Grown in the Ordered State," J. Appl. Phys. 35, 3320 (1964).

2. A. J. Pointon and J. M. Robertson, "The Growth of Large Single Crystals of Lithium Ferrite," J. Materials Science, 2, 293 (1967).

3. D. A. Lepore, R. J. Belt, and J. W. Nielsen, "Dependence of Ferromagnetic Resonance Linewidth on Structural Defects in Single Crystals of Lithium Ferrite," J. Appl. Phys. 38, 1421 (1967).

4. G. R. Pulliam, "Epitaxial Ferromagnetic Oxides," Autonetics Report TM3043-50-39, dated April 3, 1962.

5. G. R. Pulliam, J. E. Mee, J. L. Archer, and R. G. Warren, "Epitaxial Ferrite Memory Planes," Proc. National Aerospace Electronics Conference, IEEE, New York 1965.

6. J. L. Archer, G. R. Pulliam, R. G. Warren, and J. E. Mee, "Chemical Vapor Deposition of Single Crystal Metal Oxides. II. Encapsulation of Polycrystalline Conductors in Single Crystal Ferrite," Crystal Growth, H. Peiser, Editor, Pergamon Press, New York (1967).

7. J. L. Archer, G. R. Pulliam, J. E. Mee, "Epitaxial Ferrite Memory Planes," Final Report, Contract AF33(615)-3969, Technical Report AFAL-TR-67-165, Oct. 1967.

8. G. R. Pulliam, "Chemical Vapor Growth of Single Crystal Magnetic Oxide Films," Invited paper at Twelfth Annual Conference on Magnetism and Magnetic Materials, November 15-18, 1966, Washington, D.C., Proceedings published in J. Appl. Phys. 38, 1120 (1967).

9. G. R. Pulliam, R. G. Warren, R. E. Holmes, and J. L. Archer, "Localized Doping of Epitaxial Ferrite Films," J. Appl. Phys. 38, 2192 (1967).

10. H. Takei and S. Takasu, "Single Crystal Film of Ferrites," Japan J. Appl. Phys. 3, 175 (1964).

11. J. E. Mee, J. L. Archer, R. H. Meade, and T. N. Hamilton, "Chemical Vapor Deposition of Epitaxial YIG on YAG and Epitaxial GdIG on YAG," Appl. Phys. Letters 10, 289 (1967).

12. J. E. Mee, "Chemical Vapor Deposition of Epitaxial Garnet Films," IEEE Vol. MAG-3, No. 3, 190 (1967).

13. R. E. Cech and E. I. Alessandrini, "Preparation of FeO, NiO, and CoO Crystals by Halide Decomposition," Trans. Am. Soc. Metals 50, 150 (1959).

14. P. S. Schaffer, "Vapor-Phase Growth of Alpha Alumina Single Crystals," J. Amer. Ceram. Soc. 48, 508 (1965).

15. J. E. Mee and G. R. Pulliam, "Chemical Vapor Deposition of Single Crystal Metal Oxides, I. MgO on MgO," in Crystal Growth, H. Peiser, Editor, Pergamon Press, New York (1967).

16. G. I. Frolov, N. M. Salanskii, Ya. A. Zaionchkowskii, V. V. Lyukshin, B. P. Trubitsyn, and Yu. V. Utkin, "Pulse Switching of Single-Crystal Ferrite Films," English Translation of Bull, Acad. Sciences USSR - Physical Series Vol. 31, No. 3, 435 (1967).

17. Masshiro Nagasawa, Shigeo Shionoya, and Shoji Makishima, "Vapor Reaction Growth of SnO_2 Single Crystals and Their Properties," Japan J. Appl. Phys. 4, 195 (1965).

18. Todashi Takashashi, Atsuko Ebina, and Akira Kamiyama, "Vapor Reaction Growth of ZnO Single Cystal," Japan J. Appl. Phys. 5, 560 (1966).

19. E. A. Weaver, "Vapor Phase Growth of ZnO Single Crystals," J. Crystal Growth 1, 320 (1967).

20. J. Noack, "Darstellung Orientierter Aufwachsungen mit Hilfe Chemischer Transportreaktionen," Z. Physik Chem. 219, 417 (1962).

21. Z. Hauptman, "The Growth of Crystals by the Chemical Transport of Material. I. A New Method of Preparing Magnetite Single Crystals," Czech. J. Phys. 12, 148 (1962).

22. P. Kleinert, "Uber die Darstellung kristallisierter stochiometrischer Ferrite durch Kombination von chemischer Transportreaktion mit der Spinellsynthese," Z. Chem. 4, 434 (1964).

23. B. J. Curtis and J. A. Wilkinson, "Preparation of Mixed Oxide Crystals by Chemical Transport Reactions," J. Amer. Ceram. Soc. 48, 49 (1965).

24. C. van de Stolpe, "Preparation of NiO Single Crystals by Chemical Transport," J. Phys. Chem. Solids, 27, 1952 (1966).

25. L. B. Robinson, W. B. White, and Rustum Roy, "Growth of Transition Metal Oxide Crystals by Halide Vapour Hydrolysis," J. Materials Sci. 1 336 (1966).

26. R. J. Stokes, T. L. Johnston, and C. H. Li, "Effect of Surface Conditions on the Initiation of Plastic Flow in Magnesium Oxide," Trans. AIME 215, 437 (1959).

27. H. Kuhnl and W. Ernst, "Darstellung von wasserfreiem $FeCl_2$, $CrCl_2$, $FeBr_2$ und $CrBr_2$," Z. Anog. u. Allgem. Chem. 317, 84 (1962).

28. Chem. Abstracts 50, 16502d (1956), abstract of paper by N. I. Pirogove and B. V. Ershler, Zhur. Priklad. Khim. 29, 1128 (1956).

29. M. A. Bredig, "Mixtures of Metals with Molten Salts," p. 377 in Molten Salt Chemistry, edited by M. Blander, Interscience Publishers, New York, 1964.

30. L. Brewer, "The Fusion and Vaporization Data of the Halides," in Chemistry and Metallurgy of Miscellaneous Materials, edited by L. L. Quill, McGraw-Hill Book Company, New York, 1950.

31. H. Takei and S. Chiba, "Vacancy Ordering in Epitaxially-Grown Single Crystals of -Fe_2O_3," J. Phys. Soc. Japan 21, 1255 (1966).

32. J. J. Hanak and D. Johnson, "Epitaxial Growth of Metal Oxides," Paper presented to Thirteenth Annual Conference on Magnetism and Magnetic Materials, November, 1967, Boston. Proceedings to be published.

33. D. W. Strickler and Rustum Roy, "Studies in the System Li_2O-Al_2O_3-Fe_2O_3-H_2O," J. Am. Ceram. Soc. 44, 227 (1961).

34. G. T. Roome, H. A. Hair, and C. W. Gerst, "Thin Ferrite Phase Shifters for Integrated Microwave Devices," J. Appl. Phys. 38, 1411 (1967).

35. Epitaxial Growth of Ferromagnetic Garnets, sponsored by Advanced Research Projects Agency (ARPA) ARPA Order No. 807, Program Code No. 6E30, Contract AF33(615)-5244.

36. R. L. Comstock, "Magnetoelastic Coupling Constants of the Ferrites and Garnets," Proc. IEEE 53, 1508 (1965).

37. E. G. Spencer, D. A. Lepore, and J. W. Nielsen, "Measurements on Lithium Ferrite Crystals having Near-Zero Defect Concentrations," J. Appl. Phys. 39, 732 (1968).

38. T. Collins, "Temperature Dependence of the Hysteresis Properties of Polycrystalline Spinel Ferrite and Garnet Materials," IEE Transactions on Magnetics, Vol. MAG-3, p.513, September, 1967.

A. NEW TECHNOLOGY APPENDIX

"After a diligent review of the work performed under this contract, no new innovation, discovery, improvement or invention was made."